

# Performance Evaluation of Hybrid Vertical Axis Wind Turbine

Khaled.M. El-Nenaey, Yehia.A. Eldrainy, Ahmed A. Eissa and Sadek.Z. Kassab

Mechanical Engineering Department, Faculty of Engineering, Alexandria University,  
Alexandria, Egypt

## ABSTRACT

Since Savonius wind turbine is known by its self-starting ability at a low wind speed while Darrieus characterized by its high efficiency, the present study aims to combine the favor characteristics of Savonius and Darrieus turbine by producing a hybrid vertical axis wind turbine and evaluate its performance. A numerical model was built up by using ANSYS Fluent 17.1 software to simulate the flow over the wind turbine blades. The model was based on 3-dimentional, incompressible and unsteady assumptions. This numerical model was validated by comparing its results with a previous published experimental work for other researchers. The validated model was used to evaluate the performance of the hybrid turbine. Three different configurations of Savonius, Darrieus and combination of them (hybrid turbine) were compared. The simulation results showed that vertical axis hybrid turbine which its Savonius rotor is located inside Darrieus rotor hybrid VAWT can achieve a higher starting torque than that of a conventional Darrieus, Savonius type VAWT. Besides at high Tip Speed Ratio (TSR) the hybrid take advantage of its drag type blades as a guide for the flow to Darrieus blades.

**Keywords:** Vertical axis wind turbines; CFD; Hybrid Turbine; Numerical simulation.

## 1.0 INTRODUCTION

The wind turbines are the future of the clean energy especially the Vertical Axis Wind Turbine (VAWT) because it can provide power in the domestic and urban areas which are the most consuming in energy if they become off the grid a lot of the production of the greenhouse gases will be excluded from the ecosystem [1]. The VAWTs are much easier in designing and the matter of costing than other clean energy methods since solar energy needs a lot of batteries to store the

energy and in maintenance and in running cost. Easier than hydroelectric generation as it does not involve any changes in the marine life [2]. The main two types of the vertical axis wind turbines are Darrieus and Savonius wind turbines. Each one of them has a different principle of operation and different advantages.

The Darrieus rotor is based on a lift and drag concept which can rotate more than the available wind speed but the most weakness in Darrieus rotors is that they are not self-starting devices which needs a little assist in the first start [3]. Generally, Darrieus wind rotor is classified into curved and straight wind rotors and its most common shapes are the eggbeater and the H-type rotor [4]. The advantage of the eggbeater over H-rotor is its resisting of the bending moment that takes place due to the centrifugal force [5]. On the other hand, the eggbeater is difficult in manufacturing and expensive in designing while the straight H-rotor Darrieus turbine has a uniform angle of attack which helps in distribution of the pressure along the blade [5-7].

Savonius rotors are totally different from Darrieus in the number of blades and the shape of the design which is a concave and convex shape. Savonius blades totally depend upon the drag concept. Savonius blades contains end plate and could be a multi stage rotors which increases the performance of the turbine, also contains overlap ratio to allow air to pass through one blade to another. In addition, it has the self-starting ability which mean that the turbine can rotate at low wind speed condition to generate starting torque, this ability can be provided in Savonius wind turbine due to many reasons [8, 9]. The number of blades is one of these reasons that have an important impact in the rotor's performance. It has been proved that Savonius with two blades is better than three blades as it proved that the Savonius with two blades started at low speed which is less than Savonius with three blades [1, 10]. The three bladed Savonius has more drag surfaces against the wind air flow than two bladed rotors[11]. The drag surfaces increase the reverse torque which leads to decrease the net torque working on the blades of Savonius wind turbine [10]. Another reason is the shape of blades where semicircle shapes have higher drag coefficient than flat plates [12-14].

Many attempts have been done to enhance the performance of vertical axis wind turbines using guides, deflectors, stators and etc. [15]. Salleh et al. [16] highlighted the practicality of using a simple flat deflector as an augmentation device to enhance the power performance of a Savonius rotor for hydrokinetic application. Mauro et al. [17] showed that the blockage effects of the duct generate a strong overpressure upstream of the Savonius rotor. They found also that the power coefficient for ducted turbines, reached 0.4, which is far higher than the bare Savonius turbines. Many researchers enhanced the performance of the Savonius wind turbine through new design configurations and modification such as; introducing an upstream deflector and downstream baffle, changing rotor twist angle, adding two inner blades [18-20]. In the other hand, the Darrieus

wind turbine also has been modified and developed to boost its efficiency through optimization of its blades number, shape, twisted angles or introduction of an upstream stator and etc. [21-24].

Hybrid wind turbines are promising technique for enhancing the performance of vertical axis wind turbines by combining Savonius and Darrieus turbines which could lead to an increase their efficiency and self-starting ability. Kou et al. [25] developed combined type straight-bladed vertical axis Wind Turbine design with two Savonius orthogonal blades in the upper region, and an H-blade configuration in the lower turbine region. The hybrid rotor configuration was found to have good starting characteristics and better performance at a higher flow speed.

Dwiyantoro [26] proved that the hybrid vertical axis wind turbine with the shorter the inner shaft will have much better self-starting and better conversion efficiency. Gavalda et al. [27] proposed a Darrieus-Savonius hybrid system and they reported that the power coefficient could reach a maximum value of 0,35. They found that when the Savonius rotor was stopped at high Tip Speed Ratio (TSR), the turbine was able to achieve a power coefficient of 0.40. But this value is still lower than that of the original Darrieus rotor. Wakui et al. [28] developed two configurations of the Darrieus eggbeater turbine and the Savonius two-stage turbine. They found at TSR 3.51 the hybrid turbine with the Savonius rotor in the middle of the Darrieus one has a maximum power coefficient of 0.204; and at TSR 3.76 the hybrid turbine with the Darrieus rotor on top of the Savonius one has a maximum power coefficient of 0.231. Bhuyan et al. [29] contrasted the self-starting characteristics of an H-rotor and a hybrid H-Savonius VAWT. They found that in all azimuthal positions the hybrid configuration exhibits self-starting capability.

The present study aims to compares the performance and investigate the flow behavior of the hybrid wind turbine, the bare Savonius turbine and the bare Darrieus.

## **2.0 NUMERICAL SETUP**

In order to evaluate the performance of the hybrid VAWT a numerical model was built up using ANSYS Fluent 17.1. For the purpose of validation of the numerical model, its result has been compared with the experimental work of Siddiqui et al. [30, 31]. The validated model was used to simulate and describe the flow behavior of different VAWT configurations. A stand-alone Darrieus, Savonius rotor combination of them was simulated at a variation of wind speed ranged from 3 m/s to 6 m/s.

## 2.1 Physical Domain and Boundary Conditions

The physical domain, which was used for the numerical simulation, is shown in Figure 1. The dimension of the domain is 8000 mm length, 2700 mm width and a height equal to the height of the turbine. The turbine is located downstream of the domain inlet by 3000 mm. The turbine is positioning away from the domain wall to eliminate the wall effect. In addition, a sufficient distance behind the turbine is left to allow the flow to recover before the domain outlet. The boundary conditions for the VAWT are velocity inlet at the domain inlet and the outlet flow is considered at the atmospheric pressure. The domain wall and turbine blades walls are assumed to be insulated with no slip condition. The turbine is considered isothermal with no change in temperature and the density of air is constant at  $1.22 \text{ kg/m}^3$ .

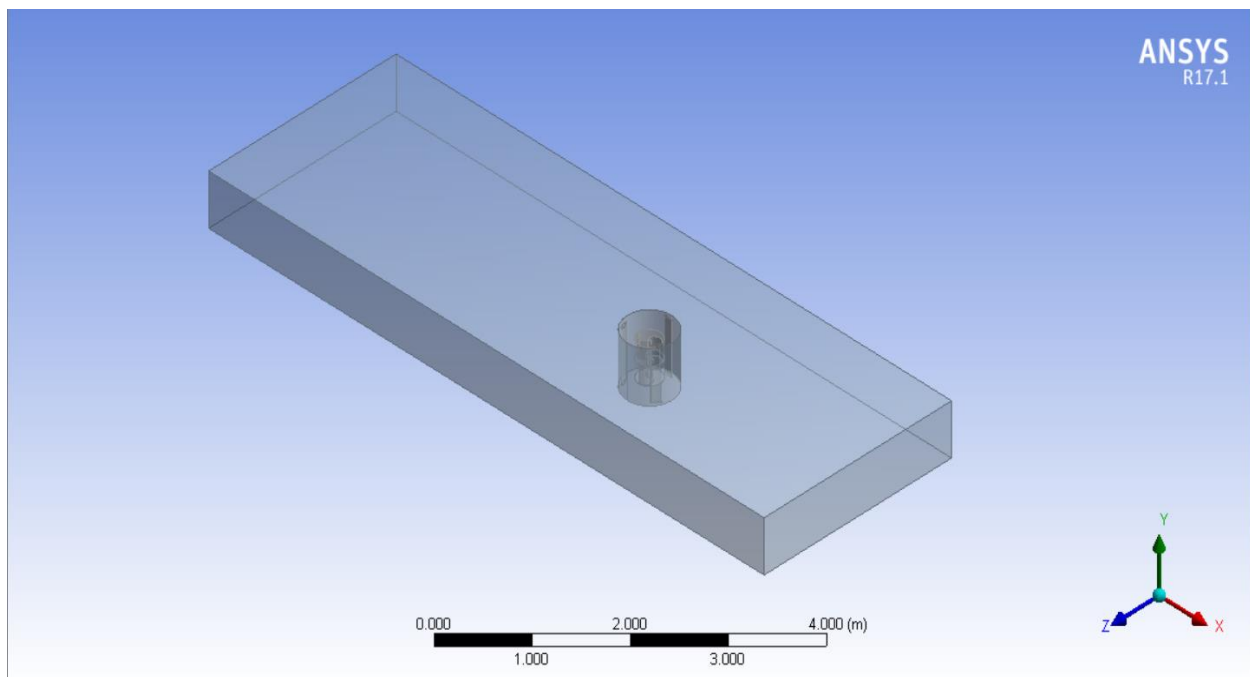


Figure 1: Three-dimensional computational domain

Three different configurations shown in Figure 2 are simulated which are a lift-type VAWT Darrieus, a drag type Savonius, and the Hybrid configuration. The Darrieus height and diameter are 660 mm 540 mm respectively and the Savonius height and diameter are 450 mm 300 mm respectively for all configurations. The Savonius wind turbine was chosen to use 2-stepped Savonius rotor, where the upper and the lower paddles pair are set at  $90^\circ$  to each other. The Darrieus has a three bucket H-rotor with DUW200 airfoil. While in the hybrid design, the savonius rotor is put middle of the Darrieus H-rotor.

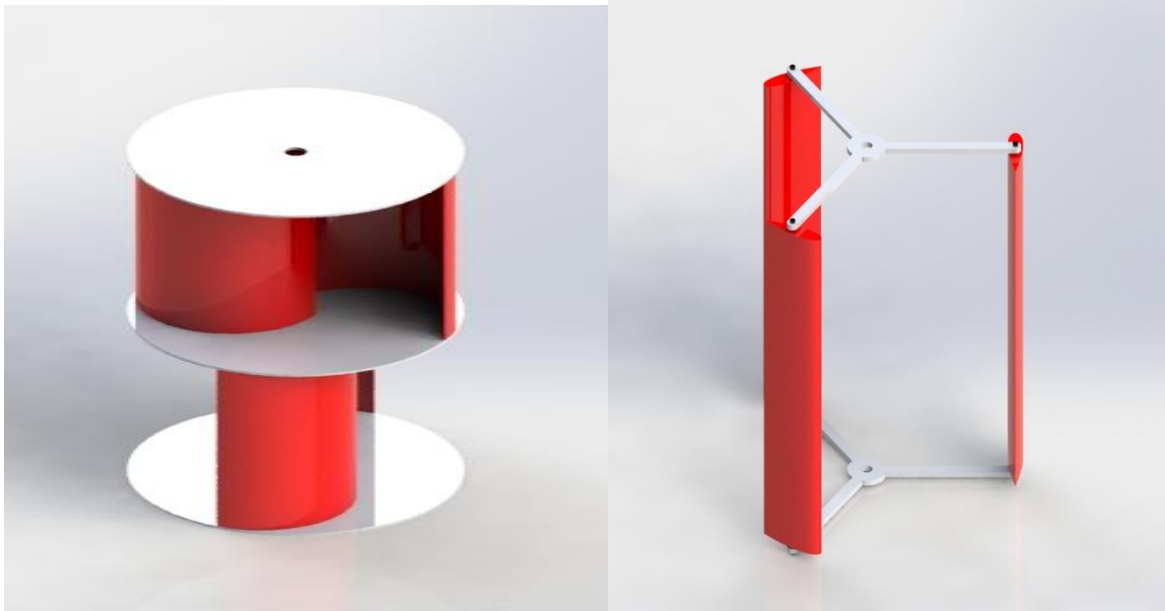


Figure 2 Different VAWT configurations

## 2.2 Mesh Generation

The current geometry is complex so that an unstructured tetrahedron mesh was used for this study. Figure 3 shows the Darrieus, Savonius and the hybrid configuration meshing. In order to assess low cost and high quality, the mesh was created with variable density so that the high gradient zones adjacent to the turbine rotor has high-resolution mesh. In addition, the mesh was refined until the mesh maximum skewness of 0.801125 was achieved.

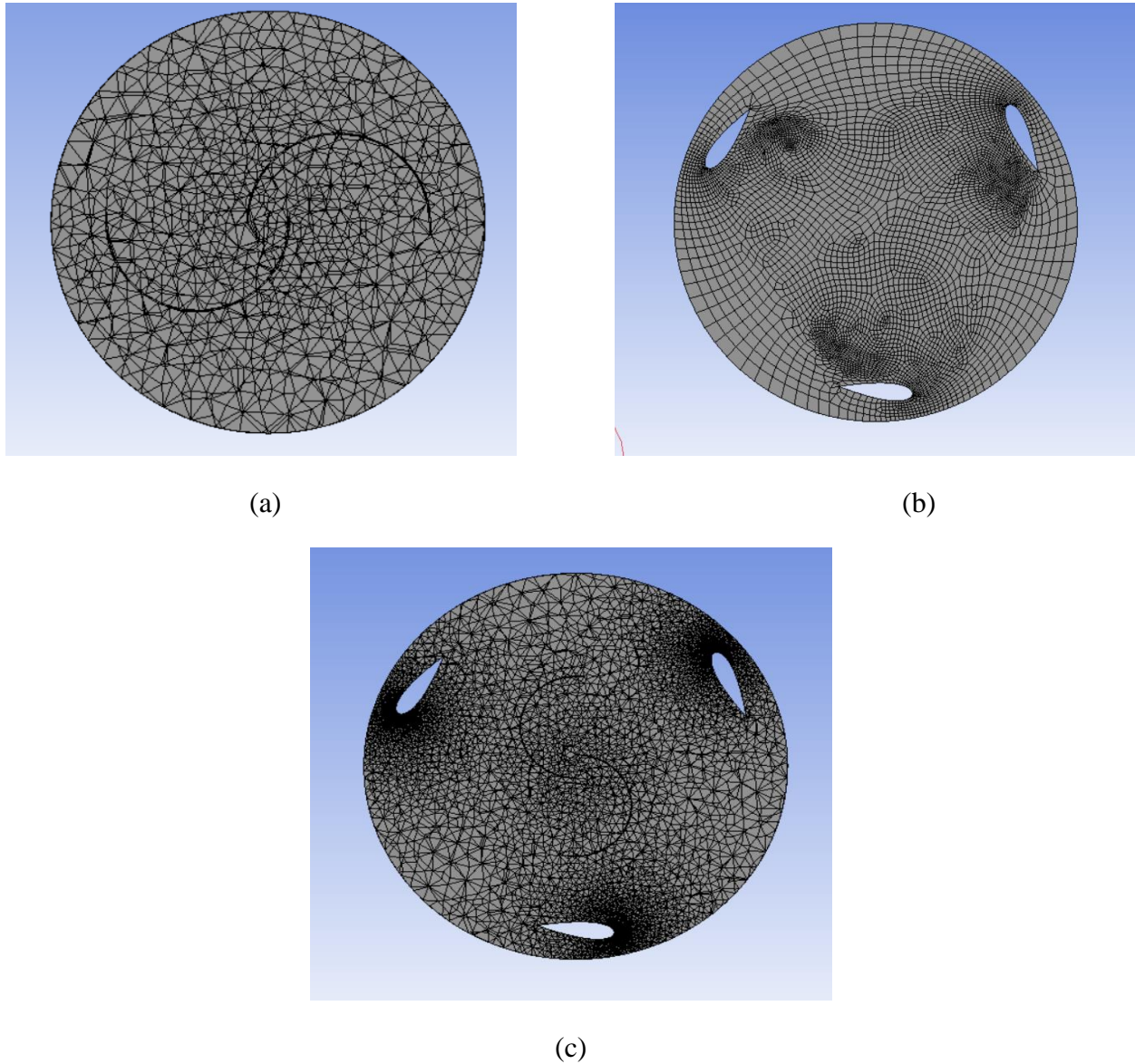


Figure 3 Meshing of different configurations (a) Darrieus, (b) Savonius and © Hybrid mesh.

The accuracy of the calculation is depending on the type and number of the mesh and its distribution which means the number and distribution of the nodes is directly proportional to the accuracy of the simulation. However, increasing the number of mesh nodes too much may not give a significant change of the simulation but it only consumes time so that, it was the purpose of the grid independence to predict the best range of number of nodes to provide the highest accuracy with the least consumption of time. The mesh independence study was performed to confirm the capability of the numerical model of capturing the flow gradient in all zones of the domain and the independence of the solution of the number of cells. Therefore, a set of nodes were taken to simulate the flow over Savonius blades, which were 25323, 41435, 72189, 107093 and 203358 nodes. The wind speed of 3 m/s was taken for all cases. A comparison of a coefficient of power (Cp) was done for all cases and it was shown from Table 1 that 107093 nodes was sufficient for an adequate solution.

Table 1 power coefficient comparison for different mesh size

Nodes number	Cp
<b>25323</b>	0.15665
<b>41435</b>	0.1575
<b>72189</b>	0.1600875
<b>107093</b>	0.165125
<b>203358</b>	0.1612485

In order to confirm the suitability of the time step to reach an acceptable solution, three cases were carried out with different time step and cell sizes. The second case time step is taken half of the first case with the same cell size. While third case number of nodes was approximately twice of the first one and time step size remains constant. Table 2 compares Cp from the three cases. The table showed last two cases seemed to approximately closed from the first case.

Table 2 Cp comparison of three simulations with different cell and time sizes

Case	First simulation	Second simulation	Third simulation
Cp	0.57	0.615	0.615

### 2.3 Numerical Model Setup.

The solution model is set using second order interpolation method for pressure, momentum, turbulent kinetic energy and turbulent dissipation rate. The realizable  $k-\epsilon$  model with enhanced wall treatment was applied to the model. The realizable  $k-\epsilon$  model has proved to be reliable and more efficient than other models [32, 33].

### 3.0 RESULTS AND DISCUSSION

For the purpose of the wind turbine to reach steady state operation all simulation cases were run until cycle to cycle variation become negligible. Figure 4 illustrates the computed moment coefficient ( $C_m$ ) which is the mean value of obtained dynamic computed moment coefficient versus the time for the hybrid turbine case at 6 m/s wind speed, it is observed that the value of  $C_m$  become almost cyclically and stabilized around a mean value with time.

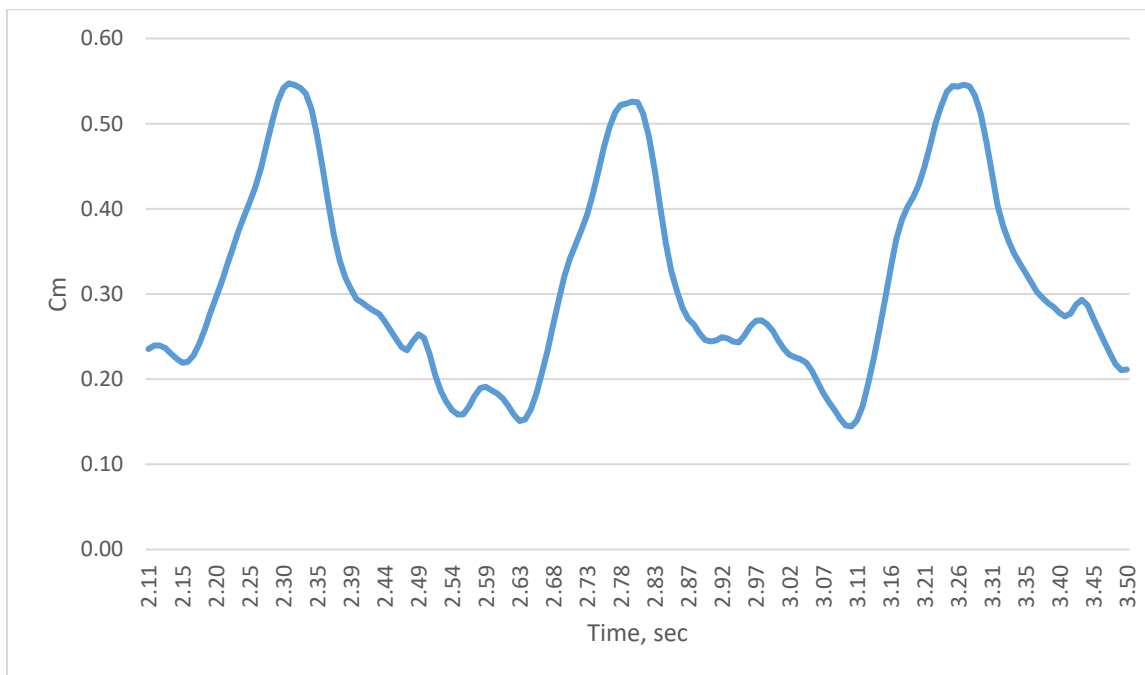


Fig. 4 Blade dynamic moment vs. time

Figure 5 shows a comparison between the present numerical results obtained from CFD simulation and experimental results by Siddiqui et al. [30, 31] of Savonius rotor in terms of power along wind speed magnitudes of 3, 5 and 6 m/s. This figure showed an excellent agreement between the two sets of results. This gives a confidence of the present numerical study.

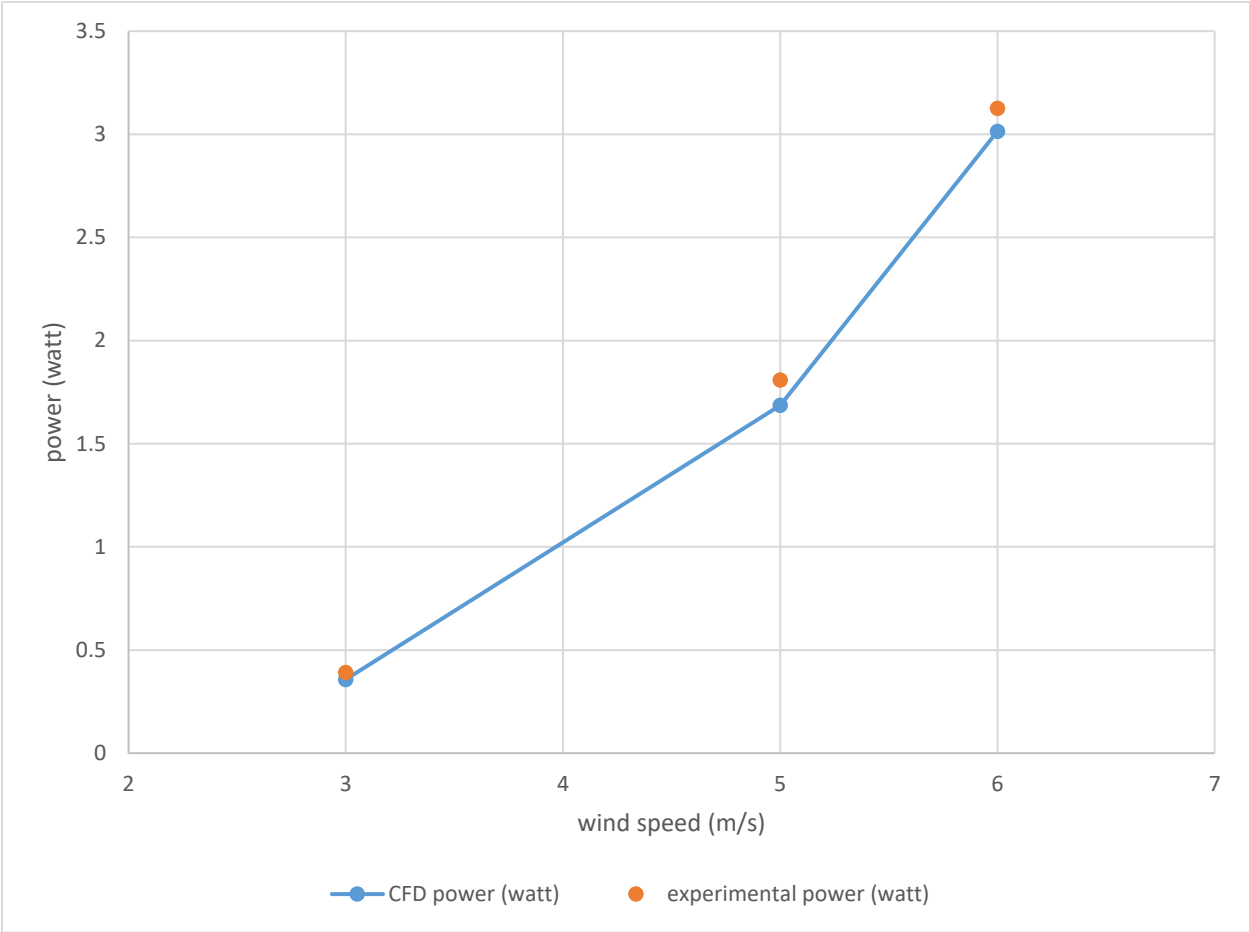


Figure 5 Comparison between the present numerical and experimental results of Siddiqui et al. [30, 31] for Savonius turbine

Figure 6 shows the variation of the output power per unit frontal area for Savonius, Darrieus, the sum of the power produced by individual Darrieus and Savonius turbines and hybrid wind turbine versus the wind speed. For certain, it is clear that the savonius turbines provide the least power, this proves that Savonius is not capable of reaching high power generation compared to the other two. Moreover, the hybrid wind rotor gives the higher power per area than the sum of power produced by individual Darrieus and Savonius turbines for the same wind speed. This owing to the improvement of air flow over the Darrieus blades which is due to the presence of the Savonius in the middle of the hybrid turbine.

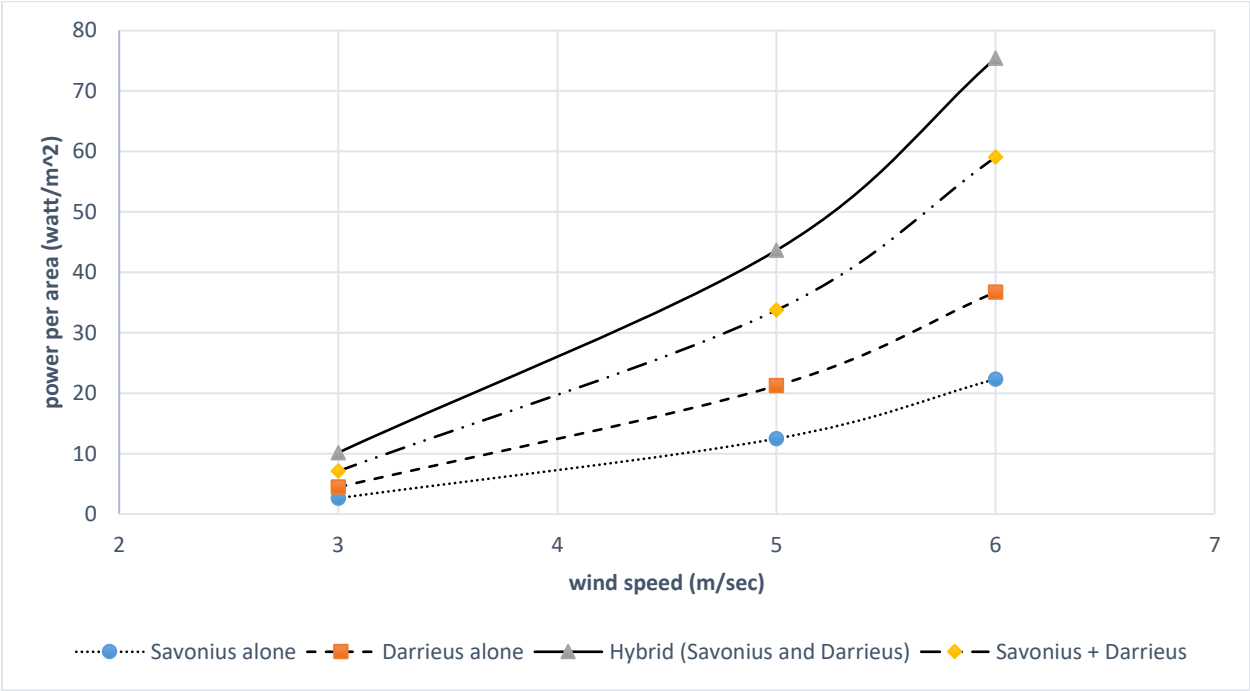


Figure 6 Comparison between variations of turbine output power per turbine frontal area at different wind speed.

In order to compare the VAWT different configurations performance, CFD simulations of the wind turbine rotating motion have been conducted at a certain wind speed. Aerodynamic characteristics of the studied wind turbines rotating at a certain speed have been achieved and the rotation speed examined in the Table 3.

Table 3 Turbine rotor rotation speed at different tip speed ratio

TSR	Savonius	Darrieus	Hybrid
0.2	76.4 rpm	42.5 rpm	42.5 rpm
1.2	458.5 rpm	255 rpm	255 rpm
1.8	687.8 rpm	382 rpm	382 rpm

Figure 7 shows a comparison of the moment coefficient for the different turbines' configuration at different tip speed ratio. The wind speed is fixed at 6 m/s while the blade speed was varied for all cases. This figure shows the ability of Savonius turbines of self-starting because it has the highest  $C_m$  at low TSR. However, as the rotating velocity increase, the generating  $C_m$  decreases. This is due to the tangential velocity of the bucket tips exceeds the flow velocity then the momentum is transferred from the turbine to the air flow, reducing the net rotor moment. Darrieus rotor has the lowest  $C_m$  at lowest TSR, as it depends on lift force. as the rotation speed increases the  $C_m$  increases until a point which  $C_m$  curve begins to go down. For the hybrid turbine, its drag-type blade can be self-starting at very low TSR. This result suggests that the lift drag hybrid turbine has the advantage of high starting torque. At TSR of 1.2 and 1.8, the hybrid turbine performs better than of the individual Savonius and Darrieus.

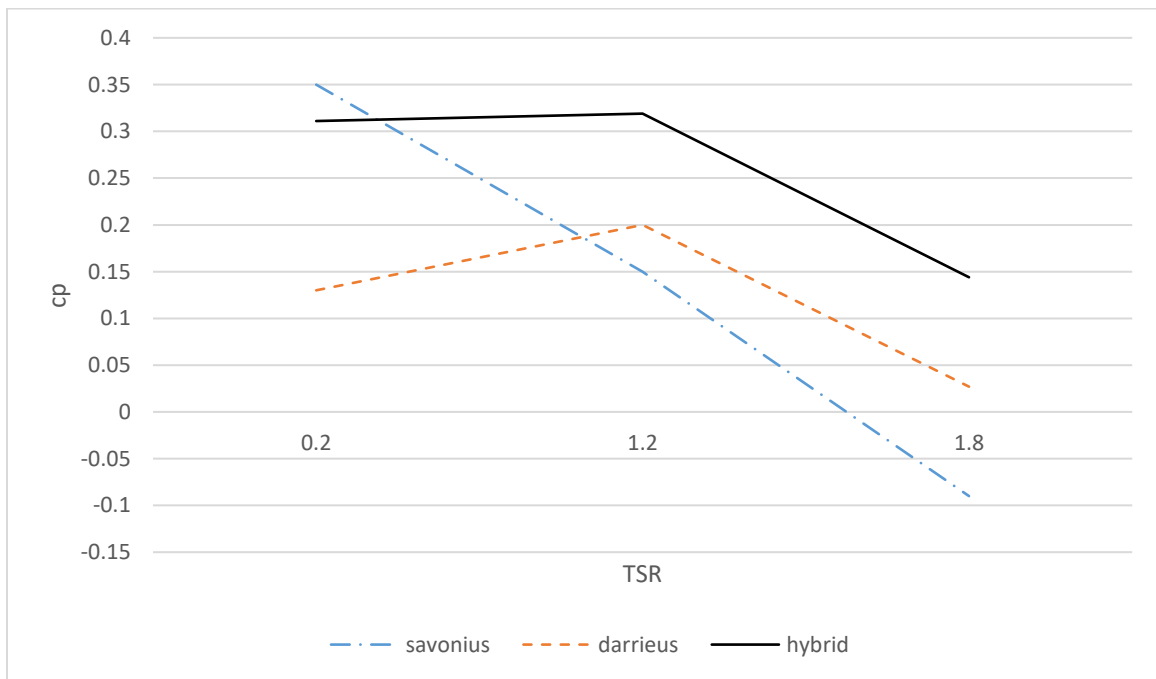


Figure 7  $C_p$  variation with the tip speed ratio

In order to support the explanation of the behaviors of different turbines and to clarify the aerodynamics behind the spinning motion of the blades, pressure distribution within the flow domain was investigated. As the wind blows into the Savonius structure as shown in Figure 8 and meets the opposite faced surfaces (one convex and other concave), a difference of a pressure force between the two surfaces results in the main driving drag force of the Savonius rotor. This figure shows the pressure contours at TSR of 0.2 in which the speed of wind is greater than the linear speed of the rotor. The position of the blades at TSR of 0.2 gives the maximum  $C_m$  value.

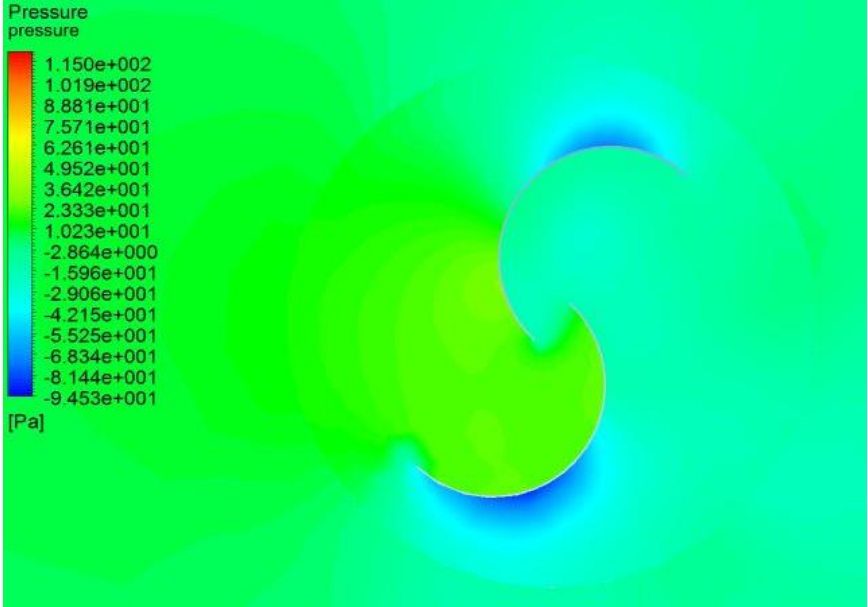


Figure 8 Savonius pressure contour at TSR Of 0.2

Figure 9 shows pressure contour of the lift type Darrieus turbine, since the blade section has a streamlined airfoil and the surface presented to the wind causes a lift force on the blade to generate a distribution of the pressure on the blade, creating a torque that causes the blades to rotate. The pressure field at the maximum aerodynamic moments occur is presented in this figure. It is observed from Figure 9 that when the aerodynamic moment reaches its maximum value, a large pressure difference between the two surfaces of the right blade drives it to move in the clockwise direction.

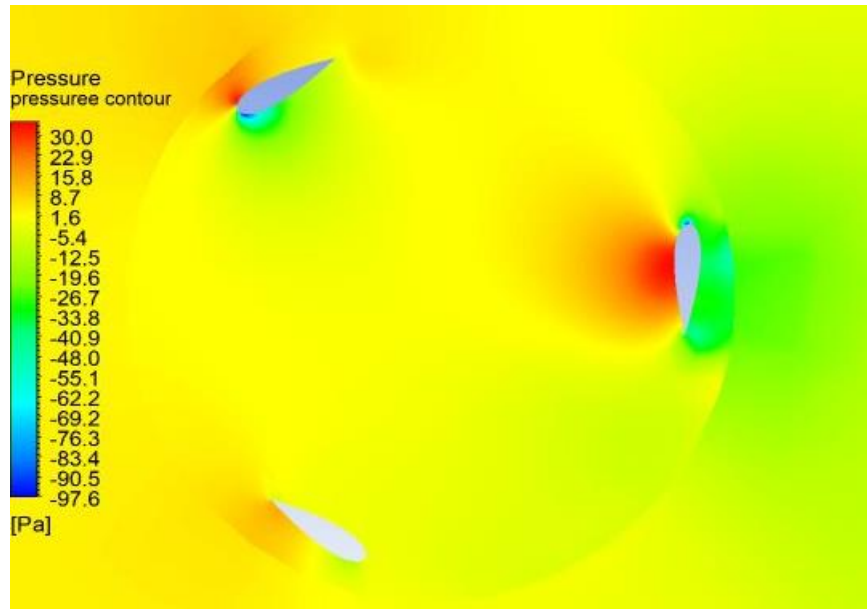


Figure 9 Darrieus pressure contour at TSR of 0.2

Figures 10 show the static pressure distribution for the hybrid wind turbine. The high difference in the pressure on both the Savonius and Darrieus blades leads to enhance the performance of the hybrid turbine than the Darrieus turbine.

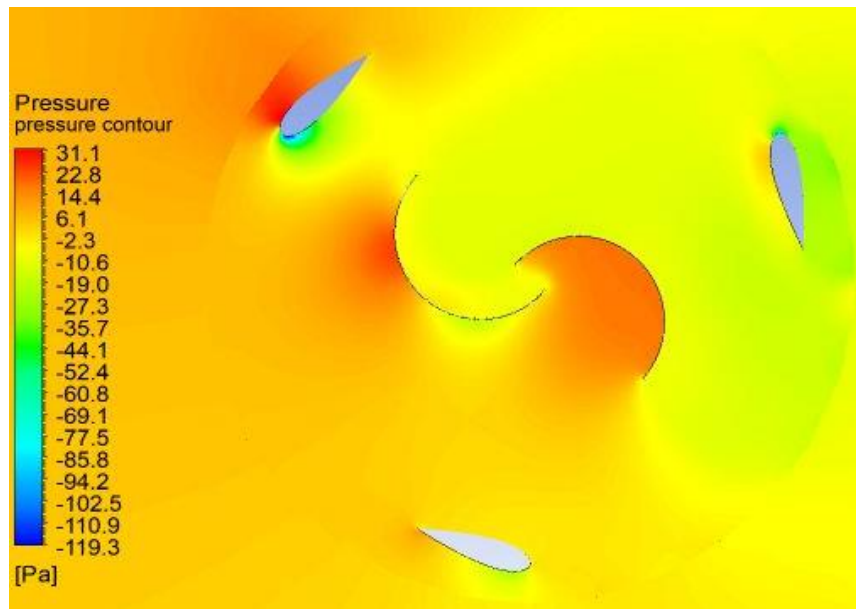


Figure 10 Hybrid pressure contour at TSR of 0.2

Figure 11 shows the Savonius turbine pressure contours at the TSR 1.8 at which the wind speed is lower than the rotor linear speed. Due to the high relative speed between the wind and blade, this position raises the drag on the blade which moves in opposite directions to a flowing wind. As shown in Figure 11, the pressure on the opposing wind blade exceeds the blade moves with the wind direction. This leads to low or a negative torques on the higher values of the tip speed ratio and hence it hinders the rotation of the Savonius turbine.

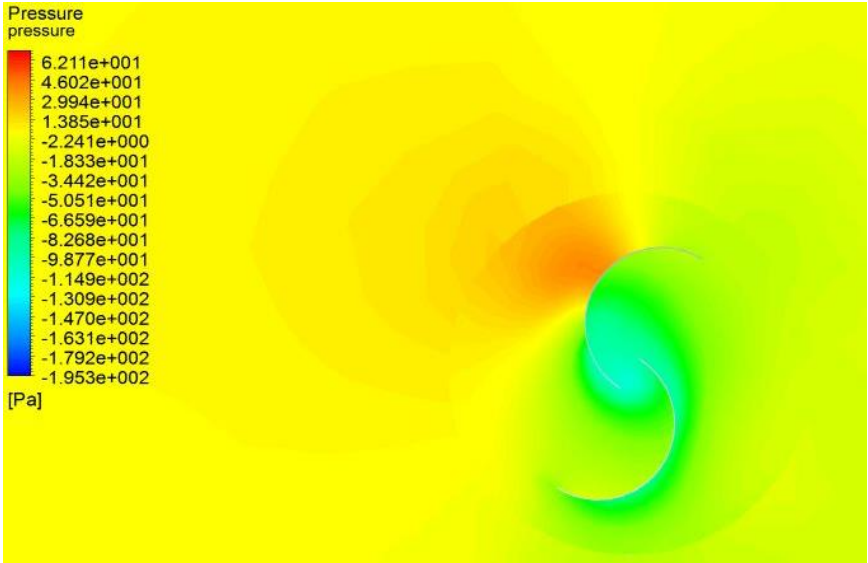


Figure 11 Savonius pressure contour at TSR Of 1.8

By contrast to Figure 9, it is observed from Figure 12 that the aerodynamic moment is decreased, when the tip speed ratio increased to 1.8. This is due to pressure difference on the region of the blade is reduced as result of the reduction of the relative speed between the flow and blade speed.

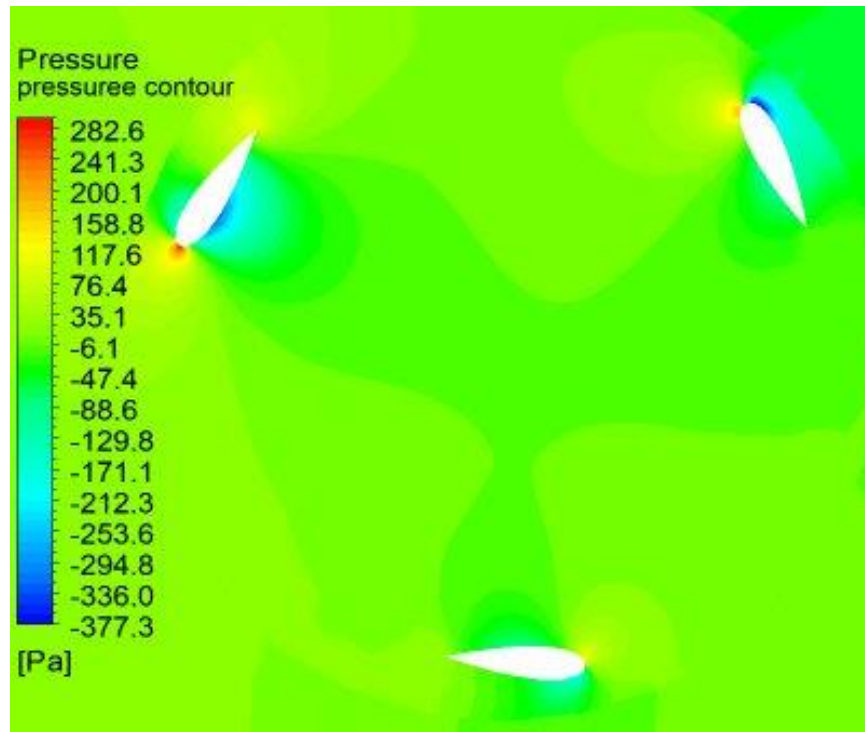


Figure 12 Darrieus pressure contour at TSR Of 1.8

Figure 13 displays the hybrid wind turbine static pressure distribution at TSR 1.8. Due to the reduction in the relative velocity available, the pressure difference in the Savonius and Darrieus blades is decrease than that for TSR 0.2. The hybrid success at this TSR is therefore better due to the presence of the Savonius blades in the center of the Darrieus blades. This directs the flow towards the Darrieus blades and boosts the hybrid turbine's overall performance.



Figure 13 Hybrid pressure contour at TSR Of 1.8

The Darrieus wind turbine streamlines at TSR of 1.8 can be seen in Figure 14. The figure shows that the flow is trapped within the turbine blades and thus results in a substantial reduction in the output power compared to the hybrid turbine. On the other hand, Figure 15 shows the streamlines at the same TSR value, and it is clear from the figure that the middle Savonius blades block the flow and direct it to the side of the Darrieus blades. As a consequence, savonius serves as a deflector so that the Darrieus blades could perform better at higher values of tip speed ratio. Therefore, the hybrid turbine performance is enhanced by taking advantage of this deflector.

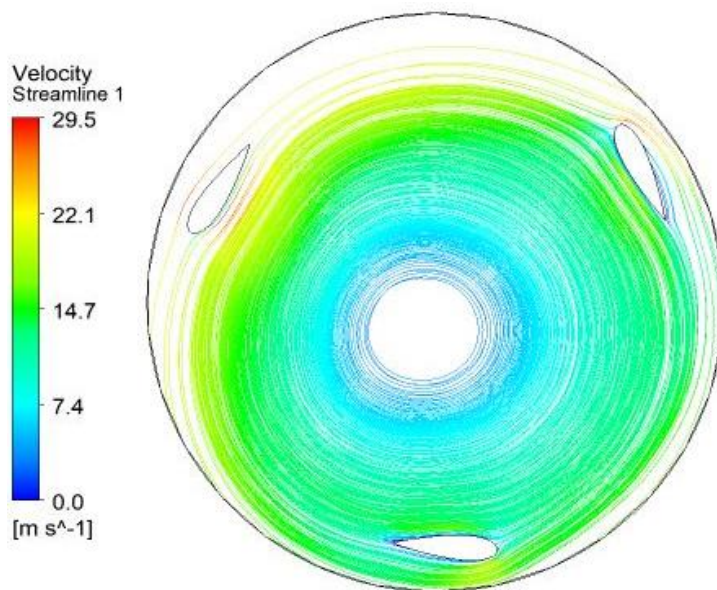


Figure 14 Darrieus particle tracking at TSR Of 1.8

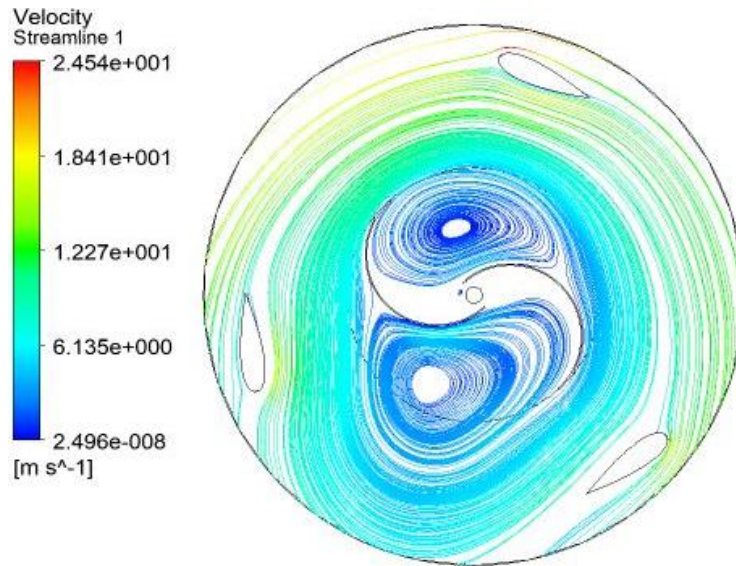


Figure 15 Hybrid particle tracking at TSR Of 1.8

## 4.0 CONCLUSION

The dimensional CFD model was implemented to investigate the behavior of the flow around three different configuration of vertical axis wind turbines which are Savonius, Darrieus and hybrid of both of them. From the CFD simulation results, it can conclude the following:

- Savonius turbines are self-starting as it can produces the highest  $C_m$  at lowest TSR.
- A Darrieus wind turbine can spin at higher blade speed than the wind speed (i.e. at a tip speed ratio greater than unity).
- At constant wind speed and different TSR, the hybrid turbines perform better than of Savonius and Darrieus.
- Savonius acts like a deflector for the Darrieus blades

This study indicates that the hybrid VAWT whose lift-type and drag-type blades are combined can achieve a higher starting torque than that of a conventional Darrieus, Savonius type VAWT. Besides at high TSR the hybrid take advantage of its drag type blades as a guide for the flow to the Darrieus.

## REFERENCES

1. Ahmed, N.A. and M. Cameron, *The challenges and possible solutions of horizontal axis wind turbines as a clean energy solution for the future*. Renewable and Sustainable Energy Reviews, 2014. **38**: p. 439-460.
2. Whittlesey, R., *Chapter 10 - Vertical Axis Wind Turbines: Farm and Turbine Design*, in *Wind Energy Engineering*, T.M. Letcher, Editor. 2017, Academic Press. p. 185-202.
3. Buchner, A.J., et al., *Dynamic stall in vertical axis wind turbines: Comparing experiments and computations*. Journal of Wind Engineering and Industrial Aerodynamics, 2015. **146**: p. 163-171.
4. Raciti Castelli, M., A. Englaro, and E. Benini, *The Darrieus wind turbine: Proposal for a new performance prediction model based on CFD*. Energy, 2011. **36**(8): p. 4919-4934.
5. Hamdan, A., et al., *A review on the micro energy harvester in Structural Health Monitoring (SHM) of biocomposite material for Vertical Axis Wind Turbine (VAWT) system: A Malaysia perspective*. Renewable and Sustainable Energy Reviews, 2014. **35**: p. 23-30.
6. Aslam Bhutta, M.M., et al., *Vertical axis wind turbine – A review of various configurations and design techniques*. Renewable and Sustainable Energy Reviews, 2012. **16**(4): p. 1926-1939.
7. Watson, S., et al., *Future emerging technologies in the wind power sector: A European perspective*. Renewable and Sustainable Energy Reviews, 2019. **113**: p. 109270.
8. Akwa, J.V., H.A. Vielmo, and A.P. Petry, *A review on the performance of Savonius wind turbines*. Renewable and Sustainable Energy Reviews, 2012. **16**(5): p. 3054-3064.
9. Kumar, A. and R.P. Saini, *Performance parameters of Savonius type hydrokinetic turbine – A Review*. Renewable and Sustainable Energy Reviews, 2016. **64**: p. 289-310.
10. Wenehenubun, F., A. Saputra, and H. Sutanto. *An experimental study on the performance of Savonius wind turbines related with the number of blades*. in *Energy Procedia*. 2015.
11. Mahmoud, N.H., et al., *An experimental study on improvement of Savonius rotor performance*. Alexandria Engineering Journal, 2012. **51**(1): p. 19-25.
12. Chen, L., et al., *Wind tunnel investigation on the two- and three-blade Savonius rotor with central shaft at different gap ratio*. Journal of Renewable and Sustainable Energy, 2016. **8**(1).
13. Mao, Z. and W. Tian, *Effect of the blade arc angle on the performance of a Savonius wind turbine*. Advances in Mechanical Engineering, 2015. **7**(5): p. 1-10.
14. Hassan Saeed, H.A., A.M. Nagib Elmekawy, and S.Z. Kassab, *Numerical study of improving Savonius turbine power coefficient by various blade shapes*. Alexandria Engineering Journal, 2019. **58**(2): p. 429-441.
15. Wong, K.H., et al., *Performance enhancements on vertical axis wind turbines using flow augmentation systems: A review*. Renewable and Sustainable Energy Reviews, 2017. **73**: p. 904-921.
16. Salleh, M.B., et al., *An experimental study on the improvement of a 2-Bladed and 3-Bladed conventional savonius rotors with a deflector for hydrokinetic application*. Journal of Advanced Research in Fluid Mechanics and Thermal Sciences, 2020. **67**(1): p. 93-102.
17. Mauro, S., et al., *CFD modeling of a ducted Savonius wind turbine for the evaluation of the blockage effects on rotor performance*. Renewable Energy, 2019. **141**: p. 28-39.
18. Youssef, K.M., et al., *An innovative augmentation technique of savonius wind turbine performance*. Wind Engineering, 2020. **44**(1): p. 93-112.
19. Zakaria, A. and M.S.N. Ibrahim. *Effect of twist angle on starting capability of a Savonius rotor - CFD analysis*. in *IOP Conference Series: Materials Science and Engineering*. 2020.
20. Al-Ghriyah, M., et al., *Performance of the savonius wind rotor with two inner blades at low tip speed ratio*. CFD Letters, 2020. **12**(3): p. 11-21.
21. Hosseini, A. and N. Goudarzi, *Design and CFD study of a hybrid vertical-axis wind turbine by employing a combined Bach-type and H-Darrieus rotor systems*. Energy Conversion and Management, 2019. **189**: p. 49-59.
22. Mahamed Sahed Mostafa Mazarbhuiya, H., A. Biswas, and K. Kumar Sharma. *Experimental Investigation on the Performance of Varying Thickness H-Darrieus Rotor*. in *Journal of Physics: Conference Series*. 2019.
23. Sengupta, A.R., A. Biswas, and R. Gupta, *Comparison of low wind speed aerodynamics of unsymmetrical blade H-Darrieus rotors-blade camber and curvature signatures for performance improvement*. Renewable Energy, 2019. **139**: p. 1412-1427.

24. Siddiqui, A.S., et al. *Experimental Study to Assess the Performance of Combined Savonius Darrieus Vertical Axis Wind Turbine at Different Arrangements*. in *Proceedings of the 21st International Multi Topic Conference, INMIC 2018*. 2018.
25. Kou, W., et al. *Modeling analysis and experimental research on a combined-type vertical axis wind turbine*. in *2011 International Conference on Electronics, Communications and Control (ICECC)*. 2011.
26. Dwiyantoro, B.A., *Computational and experimental study of optimal design on hybrid vertical axis wind turbine*. *ARPN Journal of Engineering and Applied Sciences*, 2017. **12**(20): p. 5784-5788.
27. Gavaldà, J., J. Massons, and F. Díaz, *Experimental study on a self-adapting Darrieus—Savonius wind machine*. *Solar & Wind Technology*, 1990. **7**(4): p. 457-461.
28. Wakui, T., et al., *Hybrid configuration of Darrieus and Savonius rotors for stand-alone wind turbine-generator systems*. *Electrical Engineering in Japan*, 2005. **150**(4): p. 13-22.
29. Bhuyan, S. and A. Biswas, *Investigations on self-starting and performance characteristics of simple H and hybrid H-Savonius vertical axis wind rotors*. *Energy Conversion and Management*, 2014. **87**: p. 859-867.
30. Siddiqui, A.S., et al. *Experimental Study to Assess the Performance of Combined Savonius Darrieus Vertical Axis Wind Turbine at Different Arrangements*. in *2018 IEEE 21st International Multi-Topic Conference (INMIC)*. 2018.
31. Siddiqui, A.S., et al., *255. Experimental Investigations of Hybrid Vertical Axis Wind Turbine*. 2016.
32. Song, C., et al., *Investigation of meshing strategies and turbulence models of computational fluid dynamics simulations of vertical axis wind turbines*. *Journal of Renewable and Sustainable Energy*, 2015. **7**(3).
33. Song, C., et al., *Investigation of meshing strategy and turbulence model of CFD simulation of vertical axis wind turbine*. *Taiyangneng Xuebao/Acta Energiae Solaris Sinica*, 2016. **37**(8): p. 2080-2087.